Monte Carlo Simulation of Electron Transport in Doped Silicon

G. Kaiblinger-Grujin, H. Kosina, and S. Selberherr
Institute for Microelectronics, TU-Vienna
Gusshausstrasse 27-29
A-1040 Vienna, Austria

Abstract

We present a new theoretical approach to study the electron transport in doped silicon under low electric fields. The charge distribution of the impurities is described by the Thomas-Fermi theory in the energy functional formulation. We have included many-particle effects, such as dynamical screening and multiple scattering, which become important in heavily doped semiconductors. Analytical expressions for the scattering cross section for various species of dopants using the Born approximation up to second order are derived. Monte Carlo simulations including all important scattering mechanism have been performed in the doping concentration range of 10^{15} *to* 10^{21} cm^{-3}. *The agreement with experimental data is excellent. The results confirm not only the experimental data of the mobility enhancement of minority electrons in degenerate silicon but also the lower electron mobility in As-doped silicon in comparison to P-doped silicon.*

1. Introduction

As semiconductor device dimensions decreasingly approach 0.1 μm, it becomes necessary to have accurate values of the majority- and minority electron mobilities in advanced semiconductor device simulation. Despite the importance of these quantities for device applications, such as bipolar transistors which are controlled by minority carrier flow in heavily doped regions, theoretical treatments are quite limited. There still remains a tendency in numerical simulation to assume that majority and minority mobilities are equal, although experiments have shown that majority- and minority mobilities may differ by a factor of 3 in heavily doped silicon [7][10][13][18].

Moreover, there is no theoretical model to date, which explains the different mobility data for As- and P-doped silicon for impurity concentrations higher than 10^{18} cm^{-3}. The difference between the electron mobility in As- and P-doped samples monotonically increases from 6 % at $N_I = 10^{19}$ cm^{-3} up to 32 % for $N_I = 4 \cdot 10^{21}$ cm^{-3} [12]. Ignoring these phenomena can lead to incorrect interpretation of device data which strongly depend on doping concentration.

Many attempts in the past failed to explain these differences. Ralph et al. [15] introduced a central-cell scattering potential determined empirically using bound state energies of donors. Later, El-Ghanem and Ridley [8] employed a square-well impurity core potential. Both approaches were too crude to explain the experiments sufficiently. Bennett and Lowney made extensive studies of the majority- and minority electron mobility in Si [1][2][3] and GaAs [11]. They used phase shift analysis to calculate the ionized impurity scattering cross sections of minority and majority electron scattering. As they introduced many parameters to explain experimental data for different donors, the theoretical situation remains unsatisfactorily from a physical point of view. In the well-known Brooks-Herring (BH) approach [4] the impurity's charge distribution is treated as a point charge and screening by valence electrons of the solid is neglected. Hence, the standard BH theory is not able to explain the above mentioned experimental observations.

The basis of our theoretical model is the Thomas-Fermi (TF) theory [9][19]. This semi-classical treatment of the atom in the energy functional formulation yields the impurity charge density as a function of the atomic and electron number as well as a variational parameter which defines the size of the valence electron charge cloud. Knowing the charge density we obtain analytical expressions for the cross section using the Born formalism up to second order to account for the charge sign of the impurity center [5]. This approach from first principles explains the dependence of the electron mobility on the impurity element. To our knowledge this is the first physical based model which explains the lower electron mobility in As-doped silicon than that in P-doped silicon for concentrations higher than 10^{18} cm^{-3}. As all relevant quantities are calculated analytically, the computational burden is not higher than for the simple BH model, so that this approach is well suited for device simulation.

0-8186-7901-8/97 $10.00

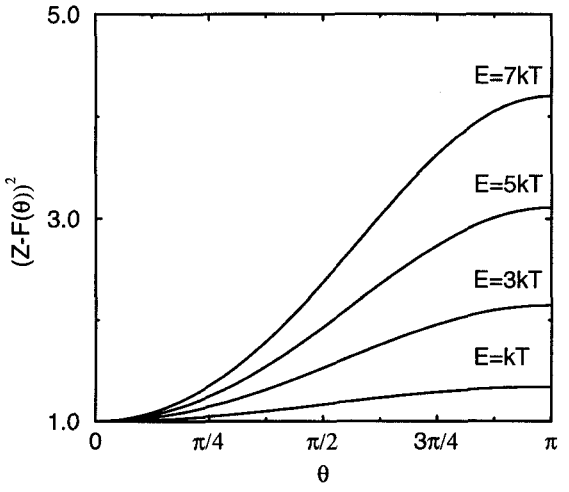

Figure 1. $[Z - F(\theta)]^2$ **for P-doped Si.**

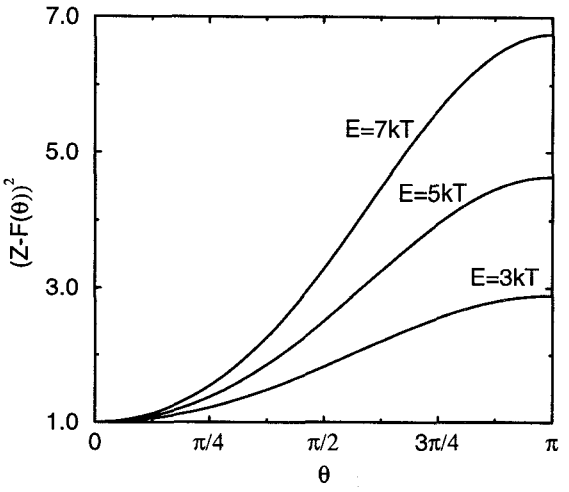

Figure 2. $[Z - F(\theta)]^2$ **for As-doped Si.**

2. Charge Density of Ionized Impurities

The total charge density (in units of the electron charge e_o) of an impurity atom with atomic number Z and electron number N in a solid is given by

$$\rho_{ion}(r) = Z\delta(r) - \rho_e(r) \quad (1)$$

$$N = \int \rho_e(\vec{r}) d^3r \quad (2)$$

The first term in (1) describes the nuclear charge density distribution concentrated in the origin, and $\rho_e(r)$ is the electron charge density of the impurity ion. The atomic form factor $F(q)$, which represents the distribution of the valence electrons in momentum space, is defined as the Fourier transform of the charge density [14]:

$$F(q) = \int d\vec{r} \, e^{-i\vec{q}\cdot\vec{r}} \rho_e(\vec{r}) \quad (3)$$

The momentum dependent form factor strongly influences the scattering strength of the ionized impurity. Fig. 1 shows $\left(Z - F(\theta)\right)^2$ for P-doped Si for different energies assuming a screened Coulomb charge density (see next section). Only in the forward direction ($q = 0$) $F(q)$ becomes a constant equal to the number of electrons (BH limit). Yet, with increasing doping concentraton and carrier energy the angle-dependence of the atomic form factor becomes important. A similar effect shows Fig. 2 for As-doped Si with a even stronger angle dependence on the form factor which explains the lower electron mobility for As-doped Si compared to P-doped samples. From Fig. 5 we see the more complicated functional behavior of the form factor in B-doped Si which emphasizes the importance of the atomic form factor for the correct description of minority electron transport. Note that $\left(Z - F(\theta)\right)^2$ is smaller than unity in case of acceptor ions in contrast to donor ions where this factor is greater than one. At a scattering angle of $\theta = \frac{\pi}{2}$ the scattering cross section is even zero! Since the impurity ion in a solid is screened by free carriers, the effective potential in momentum space in the random phase approximation is

$$\mathcal{U}(q) = V_0 \frac{Z - F(q)}{q^2 + \beta^2 G(q)}$$

$$V_0 = \frac{2m^*}{\hbar^2} \frac{e_o^2}{\epsilon_{Sc}} \quad (4)$$

where ϵ_{Sc} is the dielectric constant of the semiconductor, and β the inverse Debye screening length which is given by

$$\beta^2 = \frac{n\, e_o^2}{\epsilon_{Sc}\, k_B\, T} \quad (5)$$

kT is the thermal energy, q the momentum transfer, and n the free carrier concentration (no compensation is assumed). The screening function $G(q) \leq 1$ represents the dielectric response of the conduction electrons to an external charge (dynamical screening). In the BH approach $G(q) = 1$ is assumed (static screening). This assumption becomes questionably in highly doped semiconductors, such as silicon at a doping concentration of $10^{18}\,\mathrm{cm}^{-3}$.

3. The Thomas-Fermi Atomic Model

To this end the only unknown quantity is the exact charge density distribution of the impurity ion in a solid. There are numerous rather sophisticated methods to calculate the electron charge density distribution. As we are interested

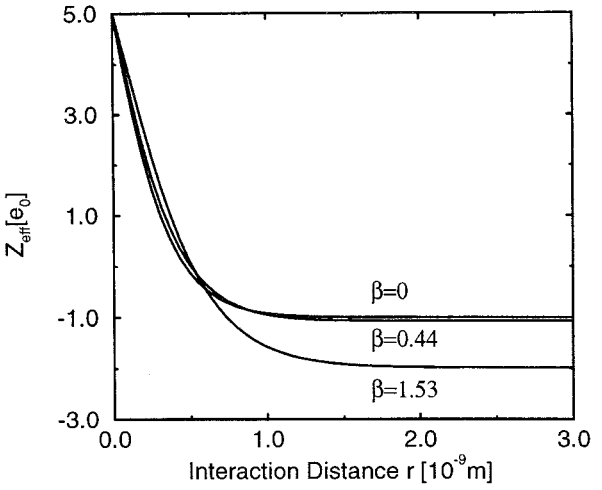

Figure 3. Z_{eff} for various inverse screening lengths β in B-doped Si.

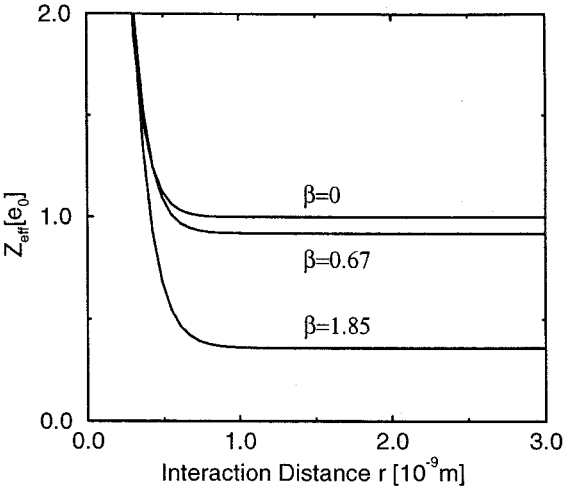

Figure 4. Z_{eff} for various inverse screening lengths β in P-doped Si.

in analytical solutions, we use the semi-classical TF model. Its basic idea is to treat the valence electrons as a degenerate Fermi gas of nonuniform, spherically symmetric electron density in a positive charged background [17] at zero temperature. Under this assumption we get a local relation between the electron charge density and the Fermi energy. The total energy consists of the classical Coloumb potential energy of electron-electron E_{e-e} and electron-nucleus interactions E_{e-n}, the kinetic energy E_k, an inhomogeneity correction E_w^{inh} [20] for the kinetic energy, and a quantum mechanical exchange energy correction [6]. Hence we define the total energy functional ($\hbar = m = 1$)

$$E_0 = E_k + E_w^{inh} + E_{e-n} + \lambda \left(E_{e-e} + E_{ex}\right) \quad (6)$$

$$E_k = c_k \int \rho_e(r)^{5/3} d^3r \quad (7)$$

$$E_{e-n} = -\frac{Z}{\epsilon_{Sc}} \int \frac{\rho_e(r)}{r} d^3r \quad (8)$$

$$E_{e-e} = \frac{1}{2\,\epsilon_{Sc}} \int\int \frac{\rho_e(r)\rho_e(\vec{r'})}{\mid \vec{r} - \vec{r'} \mid} d^3r\, d^3\vec{r'} \quad (9)$$

$$E_{ex} = \frac{c_{ex}}{\epsilon_{Sc}} \int \rho_e(r)^{4/3} d^3r \quad (10)$$

$$E_w^{inh} = \frac{1}{72} \int \frac{\left(\nabla \rho_e(r)\right)^2}{\rho_e(r)} d^3r \quad (11)$$

$$c_k = \frac{3}{10}\left(3\pi^2\right)^{2/3} \quad (12)$$

$$c_{ex} = -\frac{11}{12}\left(\frac{3}{\pi}\right)^{1/3} \quad (13)$$

In (6) λ represents the correlation parameter. In principle any function can be chosen as long as it vanishes at infinity and the integral over a certain domain remains finite. Two widely used charge density distributions (atomic form factors) are the normalized hydrogen-like exponential charge distribution

$$\rho_e(r) = \frac{N\,\alpha^3}{8\pi} \mathrm{e}^{-\alpha\, r} \quad (14)$$

$$F(q) = \frac{N\alpha^4}{(q^2+\alpha^2)^2} \quad (15)$$

and the normalized screened Coloumb charge distribution:

$$\rho_e(r) = \frac{N\,\alpha^2}{4\pi} \frac{\mathrm{e}^{-\alpha\, r}}{r} \quad (16)$$

$$F(q) = \frac{N\alpha^2}{q^2+\alpha^2} \quad (17)$$

The corresponding scattering potential can be written as

$$V(r) = -\frac{Z_{eff}}{\epsilon_{Sc}} \frac{\mathrm{e}^{-\beta\, r}}{r} \quad (18)$$

with the effective charge

$$Z_{eff} = Z - N^* \left(1 - \mathrm{e}^{-(\alpha-\beta)r} \left(1 - \frac{\left(\beta^2 - \alpha^2\right)\, r}{2\,\alpha}\right)\right)$$

$$N^* = \frac{N}{\left(1 - \frac{\beta^2}{\alpha^2}\right)^2} \quad (19)$$

for an exponential distribution and

$$Z_{eff} = Z - \frac{N}{1 - \frac{\beta^2}{\alpha^2}} \left(1 - \mathrm{e}^{-(\alpha-\beta)\, r}\right) \quad (20)$$

for a screened Coulomb charge density. Fig. 3 shows the dependence of the effective charge on the impurity concentration in B-doped Si. Only for $\beta = 0$ (no screening) one obtains unity for $r \to \infty$, but in all other cases the scattered electron interacts with an negative effective charge which is always smaller that unity. Whereas in Fig. 4 one can see that the effective charge in P-doped Si becomes smaller than unity with increasing impurity concentration which explains the slower decrease of the majority electron mobility for highly doped silicon. Both density distributions have a better behavior for large r than the exact solution of the TF equation which decreases too slowly. Calculating the first derivative of the total energy with respect to the variational parameter α and the electron number N we get two equations for α and λ:

$$0 = \frac{\partial E}{\partial \alpha} \tag{21}$$

$$0 = \left.\frac{\partial E}{\partial N}\right|_{N=Z} \tag{22}$$

The latter equation is obtained from the vanishing chemical potential for a neutral atom in the TF model. Solving (21) and (22) with respect to λ and α we obtain α and λ as a function of Z and N. Substituting α and λ in (6) we obtain for the total energy functional in case of an exponential density

$$E_0 = c_k^* N^{5/3}\alpha^2 + \frac{N\alpha^2}{72} - \frac{NZ\alpha}{2\epsilon_{Sc}} + \lambda\left(\frac{5N^2\alpha}{32\epsilon_{Sc}} + \frac{c_{ex}^*}{\epsilon_{Sc}} N^{4/3}\alpha\right) \tag{23}$$

and

$$E_0 = c_k^* N^{5/3}\alpha^2 - \frac{NZ\alpha}{\epsilon_{Sc}} + \lambda\left(\frac{N^2\alpha}{4\epsilon_{Sc}} + \frac{c_{ex}^*}{\epsilon_{Sc}} N^{4/3}\alpha\right) \tag{24}$$

for a screened Coulomb density.

4 Scattering Rate

The differential cross section in the first Born approximation can be written as:

$$\frac{d\sigma_{B1}}{d\Omega} = |\mathcal{U}(q)|^2 \left(1 + \frac{\sin(qR)}{qR}\right) \tag{25}$$

The term in brackets takes into account the scattering of an electron on pairs of ionized impurities. The average separation R between neighboring impurities is defined as [16]

$$R \equiv \langle r \rangle \approx (2\pi N_I)^{-\frac{1}{3}} \tag{26}$$

The total cross section $\sigma_t(k)$ is the integral of (25) over the solid angle. The total impurity scattering rate is defined as

$$\lambda(k) = \frac{N_I \hbar k}{m^*} \sigma_t(k) \tag{27}$$

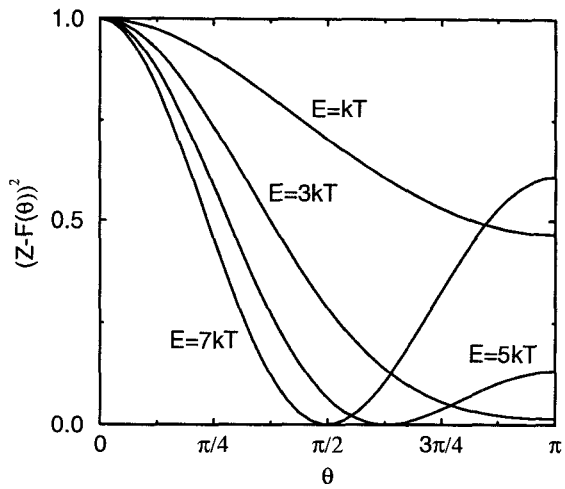

Figure 5. $[Z - F(\theta)]^2$ **for B-doped Si.**

with

$$\sigma_t(k) = \sigma_{B1}(k) + \sigma_c(k) \tag{28}$$

The selection of a impurity scattering process can be computed by a rejection method. σ_c is a correction of third order in the interaction strength V_0 including the second Born amplitude which is defined for a point charge with $F(q) = N$ as

$$\begin{aligned} f_2(q) &= \frac{{U_0}^2}{qA(q)}\left(\operatorname{atan}\left(\frac{\beta q}{2A(q)}\right) + \frac{i}{2}\log\frac{A(q)+kq}{A(q)-kq}\right) \\ A(q) &= \sqrt{\beta^4 + 4\beta^2 k^2 + k^2 q^2} \\ U_0 &= \frac{2m^*(Z-N)}{\hbar^2} \cdot \frac{e^2}{\epsilon_{Sc}} \end{aligned} \tag{29}$$

As a consistent derivation of the second Born amplitude including dynamic screening is impossible, we set the screening function equal to unity. For the same reason we drop the two-ion correction. Using (27) in a Monte Carlo simulator enables us to calculate the local average electron drift velocity v_d. We obtain the electron drift mobility using the relation

$$\mu = \frac{v_d}{|\vec{E}|} \tag{30}$$

5. Results and Discussion

As an example we present results for silicon at room temperature. All impurities are assumed to be ionized. In addition to ionized impurity scattering which is the main

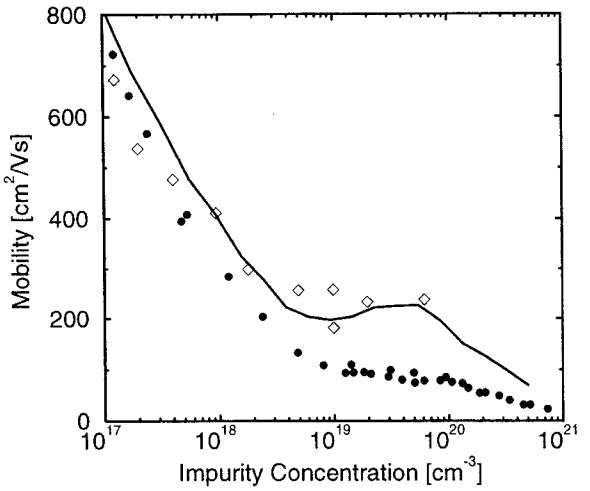

Figure 6. Minority electron mobility in B-doped Si: Simulation: solid line; experimental data from [18]: open diamonds; compared to the majority mobility: filled circles [12].

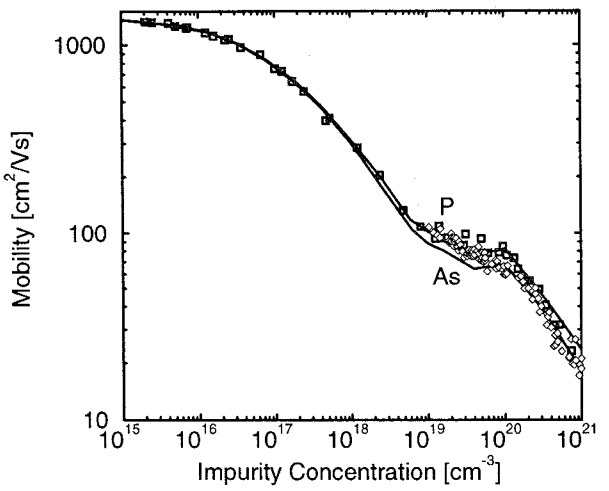

Figure 7. Majority electron mobility in P- and As-doped Si over the full doping range. Simulation: solid lines; experimental data from [12]: open diamonds (As); open squares (P).

scattering process in heavily doped semiconductors, we take into account phonon scattering and electron-plasmon scattering. The latter effect lowers the mobility in p-type material significantly and is responsible for the dip in the minority mobility at about $N_I = 10^{19}$, which corresponds to the maximum strength of the electron-plasmon interaction. At those concentrations degeneracy effects are strong; therefore we include the Pauli exclusion principle (majority electrons only) and the Fermi-Dirac statistics in our calculations. Calculated ground state energies of different ions and neutral atoms with a hydrogen-like density function give extremely accurate results (within 2 %) in comparison with experimental data. From Figs. 3 and 4 one can see that with increasing doping level the BH approach of a constant effective impurity charge becomes wrong (cf. Figs. 1,2 and 5). Only when the distance from the impurity becomes infinite and the screening length equals zero (i.e. no screening and a structureless impurity ion with N point-like valence electrons in the origin), we get a constant impurity charge $Z-N$. In all other cases we have $Z_{eff} < Z - N$. Figs. 1-2 and 5 show $\left(Z - F(\theta)\right)^2$ as a function of the scattering angle θ for different energies. This expression, which represents actually the effective charge in momentum space, strongly influences the scattering cross section. Only in a small doping region the BH model using the first Born approximation is valid. Note the completely different behavior for acceptor and donor-ions. In heavily doped regions screening valence electrons reduce the charge of the positive charged acceptors significantly which explains the almost constant majority electron mobility in the doping region $[4 \cdot 10^{19} - 10^{20}]$ cm^{-3} (Figs. 4, 7 and 8). On the other hand, the effective charge of the negative charged boron ion is two times higher than its original charge at $N_I = 10^{20}\,\mathrm{cm}^{-3}$ (Fig. 3) and even eight times higher at $N_I = 10^{21}\,\mathrm{cm}^{-3}$. Hence a stronger repulsion of the effective scattering potential for acceptors makes this scattering process less effective. The vanishing electron-plasmon interaction and the stronger repulsion are responsible for the increase of the minority electron mobility up to $4 \cdot 10^{19}\,cm^{-3}$ (Fig. 6) and the generally higher mobility in p-type Si. In the case of As-doped Si the effective charge remains almost unchanged even at high doping concentrations. The squared difference between Z and $F(\theta)$ is higher compared to P-doped Si for the same energy. Hence, the electron mobility is always lower in As-doped samples than in P-doped samples. (Figs. 7 and 8).

6. Conclusion

We have shown that even in the first Born approximation one can differentiate between attractive and repulsive scattering centers, if one takes into account the spatial charge distribution of the ionized impurities properly. The momentum dependence of the atomic form factor has to be considered to reproduce the dopant dependent electron mobility in heavily doped semiconductors. Hence, the failure of explaining minority- and majority electron mobilities in the past was due to neglecting the atomic form factor which is responsible for the different effective charges of the ionized dopants. Furthermore, it can be concluded that the two-ion correction is important over the whole doping range, whereas dynami-

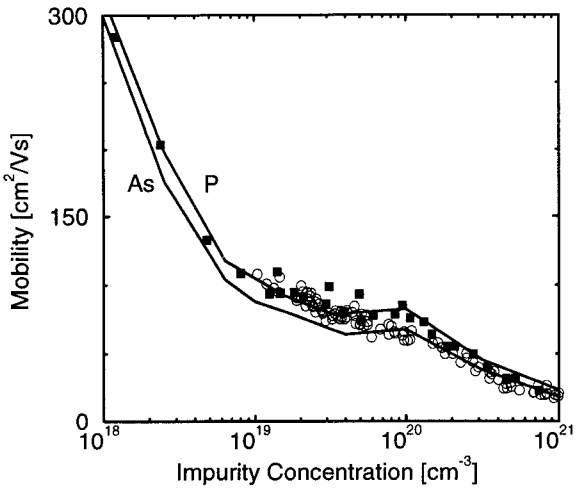

Figure 8. Majority electron mobility in P- and As-doped Si. Simulation: solid lines; experimental data from [12]: open circles (As); filled squares (P).

cal screening and the second Born correction are becoming important at $N_I = 10^{18}$. Due to the lack and inconsistency of experimental data for the minority mobility it is difficult to compare our simulation results quantitatively for this particular case. It is hoped that the results outlined here will stimulate more experimental work to establish the different electron mobilities observed for various species of donors in n- and p-type Si.

References

[1] H. Bennett. Hole and electron mobilities in heavily doped silicon: Comparison of theory and experiment. *Solid-State Electron.*, 26(12):1157–1166, 1983.

[2] H. Bennett and J. Lowney. Calculated majority- and minority-carrier mobilities in heavily doped silicon and comparisons with experiment. *J.Appl.Phys.*, 71:2285–2296, 1992.

[3] H. Bennett and J. Lowney. Majority and minority mobilities in heavily doped silicon for device simulations. In *Workshop on Numerical Modeling of Processes and Devices for Integrated Circuits NUPAD IV*, pages 123–128, Seattle, 1992.

[4] H. Brooks. Scattering by ionized impurities in semiconductors. *Physical Review*, 83:879, 1951.

[5] R. Dalitz. On higher Born approximations in potential scattering. *Proc.Roy.Soc.(London)*, A206:509–520, 1951.

[6] P. Dirac. Note on exchange phenomena in the Thomas-Fermi atom. *Proc.Camb.Philos.Soc.*, 26:376–385, 1930.

[7] J. Dziewior. Minority-carrier diffusion coefficients in highly doped silicon. *Appl.Phys.Lett.*, 35:170–172, 1979.

[8] H. El-Ghanem and B. Ridley. Impurity scattering of electrons in non-degenerate semiconductors. *J.Phys.C:Solid State Phys.*, 13:2041–2054, 1980.

[9] E. Fermi. Un metodo statistico per la determinazione di alcune priorieta dell'atome. *Rend.Accad.Naz.Lincei*, 6:602–607, 1927.

[10] I. Leu and A. Neugroschel. Minority-carrier transport parameters in heavily doped p-type silicon at 296 and 77 K. *IEEE Trans.Electron Devices*, 40(10):1872–1875, 1993.

[11] J. Lowney and H. Bennett. Majority and minority electron and hole mobilities in heavily doped GaAs. *J.Appl.Phys.*, 69(10):7102–7110, 1991.

[12] G. Masetti, M. Severi, and S. Solmi. Modeling of carrier mobility against carrier concentration in arsenic-, phosphorus- and boron-doped silicon. *IEEE Trans.Electron Devices*, ED-30(7):764–769, 1983.

[13] A. Neugroschel. Minority-carrier diffusion coefficients and mobilities in silicon. *IEEE Electron Device Lett.*, EDL-6(8):425–427, 1985.

[14] N.F.Mott and H. Massey. *The Theory of Atomic Collisions.* Clarendon Press, Oxford, 1949.

[15] H. Ralph, G. Simpson, and R. Elliot. Central-cell corrections to the theory of ionized-impurity scattering in silicon. *Physical Review*, 11(8):2948–2956, 1975.

[16] B. Ridley. *Quantum Processes in Semiconductors.* Clarendon Press, Oxford, 1993.

[17] L. Scarfone. Thomas-Fermi-type dielectric screening of statistical atomic models of donor-specific impurities in a semiconductor-like valence electron gas at zero temperature. *J.Phys.C:Solid State Phys.*, 8:5585–5602, 1996.

[18] S. Swirhun, D. Kane, and R. Swanson. Measurements of electron lifetime, electron mobility and band-gap narrowing in heavily doped p-type silicon. pages 24–27. Proc.IEDM, 1986.

[19] L. Thomas. The calculation of atomic fields. *Proc.Camb.Philos.Soc.*, 23:542–548, 1927.

[20] C. von Weizsäcker. Zur Theorie der Kernmassen. *Z.Phys.*, 96:431–458, 1935.